THE JOURNAL OF PHYSICAL CHEMISTRY B

Article

pubs.acs.org/JPCB

Separating Annihilation and Excitation Energy Transfer Dynamics in Light Harvesting Systems

Mikas Vengris,*[,†] Delmar S. Larsen,[‡] Leonas Valkunas,[§,∥] Gerdenis Kodis,[⊥] Christian Herrero,[⊥] Devens Gust,[⊥] Thomas Moore,[⊥] Ana Moore,[⊥] and Rienk van Grondelle[#]

[†]Quantum Electronics Department, Faculty of Physics, Vilnius University, Saulėtekio 9-III, 10222 Vilnius, Lithuania

[‡]Department of Chemistry, University of California Davis, One Shield Avenue, Davis, California 95616, United States

[§]Department of Theoretical Physics, Faculty of Physics, Vilnius University, Sauletekio Ave. 9-III, 10222, Vilnius, Lithuania

[∥]Center for Physical Sciences and Technology, Gostauto 9, 01108, Vilnius, Lithuania

[⊥]Department of Chemistry and Biochemistry, Arizona State University, Tempe, Arizona 85287, United States

[#]Faculty of Sciences, Vrije Universiteit Amsterdam, De Boelelaan 1081, 1081 HV Amsterdam, The Netherlands

ABSTRACT: The dependence of excitation energy transfer kinetics on the electronic state of the acceptor (ground vs excited) has been resolved with a novel multipulse prePump−Pump−Probe spectroscopy. The primary energy transfer and annihilation dynamics in two model light-harvesting systems were explored: an artificially synthesized carotenoid-zinc-phthalocyanine dyad and a naturally occurring light-harvesting peridinin-chlorophyll protein complex from *Amphidinium carterae*. Both systems use carotenoid as the primary excitation energy donor with porphyrin chromophores as the acceptor molecules. The prePump−Pump−Probe transient signals were analyzed with Monte Carlo modeling to explicitly address the underlying step-by-step kinetics involved in both excitation migration and annihilation processes. Both energy transfer and annihilation dynamics were demonstrated to occur with approximately the same rate in both systems, regardless of the excitation status of the acceptor pigments. The possible reasons for these observations are discussed in the framework of the Förster energy transfer model.

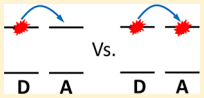

1. INTRODUCTION

It is an intrinsic feature of multichromophoric molecular aggregate systems that nonlinear multiple excitation dynamics (e.g., annihilation) can coexist with linear single-excitation dynamics (e.g., energy and electron transfer reactions).[1−4] This is especially important for studying the functioning of light harvesting photosynthetic systems consisting of numerous chromophores like chlorosomes, whereby the experimental characterization of energy transfer dynamics free of annihilation effects is often quite difficult.[5,6] Consequently, this often makes the analysis of the annihilation process necessary. However, the analysis of excitation annihilation is not just an obligatory burden arising from high laser fluences often used for the experiments; excitation annihilation dynamics results from the excitation dynamics in the molecular system, and its analysis can provide useful information about the structure of the complex under investigation and the underlying energy transfer dynamics.[4,7,8] In particular, it has been used successfully to determine excitation energy transfer (EET) pathways and rates in photosynthetic light harvesting complexes.[8−12]

Modeling nonlinear excitation annihilation dynamics is conceptually similar to modeling bimolecular chemical reactions, in the case of the singlet−singlet annihilation (A + A → A) or for singlet−triplet annihilation (A + B → B).[13] When excitation energy is transferred from an excited donor (A) to an excited acceptor molecule (A or B), the acceptor is promoted to a higher-lying excited state (S_n) that is typically short-lived and non-adiabatically internally converts to the lowest excited state, S_1 (Figure 1). The net result is that one of the original two excitations is converted to heat. As with chemical reactions, annihilation dynamics may be diffusion-limited, with the time scale dictated by the time required for two excitations to "find each other" in the molecular aggregate. Alternatively, the annihilation dynamics may be determined by the time scale of the primary energy transfer dynamics in the annihilation process (i.e., energy transfer dynamics from an *excited* donor to an *excited* acceptor). The latter case applies to the small assemblies of chromophores, where the size of the pigment aggregate is comparable to or smaller than the excitation diffusion radius. It is often observed in single-molecule and fluorescence imaging applications, where the EET can be monitored on a single chromophore pair.[14] For convenience, the terms "EET rate" and "annihilation rate" are used for the rates of energy transfer to a *ground*-state acceptor and to an *excited* acceptor, respectively.

In the weak donor/acceptor coupling limit, the rate of energy transfer can be described using the Förster mechanism expressed by the following equation:[15]

$$k_{DA} = \frac{9\ln(10)\kappa^2 c^4 \phi_D}{80\pi n^4 N_{av} \tau_D R^6} \int F_D(\omega)\alpha_A(\omega)\,\frac{d\omega}{\omega^4} \qquad (1)$$

Special Issue: Rienk van Grondelle Festschrift

Received: April 3, 2013
Revised: May 3, 2013
Published: May 10, 2013

   dx.doi.org/10.1021/jp403301c | *J. Phys. Chem. B* 2013, 117, 11372−11382

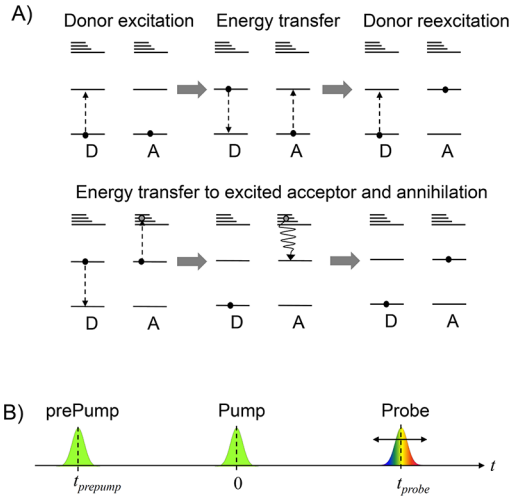

Figure 1. (A) The excitation dynamics in a hypothetical dimer consisting of a donor and an acceptor molecule: the prePump pulse creates an excitation on the donor; during the time between the prePump pulse and the Pump pulse, the excitation is transferred to the acceptor. The pump pulse produces another excitation on the donor which then annihilates with the existing excitation. The process is monitored by the probe pulse. (B) The pulse timing scheme for the prePump−Pump−Probe experiment.

where (κ^2/R^6) is the distance and orientation factor (magnitude of dipole−dipole coupling between pigments), ϕ_D is the fluorescence quantum yield of the donor, n is the refractive index of the environment, N_{av} is the Avogadro number, τ_D is the fluorescence lifetime of the donor, $F_D(\omega)$ is the fluorescence spectrum of the donor (normalized so that its integral is equal to unity), and $\alpha(\omega)$ is the absorption spectrum of the acceptor expressed in $l \cdot mol^{-1} \cdot cm^{-1}$.

The Förster equation can also be used to characterize the primary energy transfer step in annihilation, which requires substituting the **excited-state** properties of the acceptor instead of the **ground-state** properties for EET. Consequently, it is not unreasonable to expect that the EET and annihilation rates would differ significantly, since the excited-state absorption (ESA) is almost always different from the ground-state absorption (GSA) spectra. Furthermore, the transition dipole orientation of the GSA transitions are often radically different from the ESA equivalent. Experimental evidence for both the decrease and the increase of the annihilation rate vs EET rates has been reported.[14,16] To explain single molecule emission and photon antibunching observations, in some molecular aggregates, a "photon blockade" phenomenon has been proposed,[16] with the excited acceptor less likely to accept a second photon. In the other compounds, annihilation dynamics was suggested to proceed much faster than "conventional" hopping.[14]

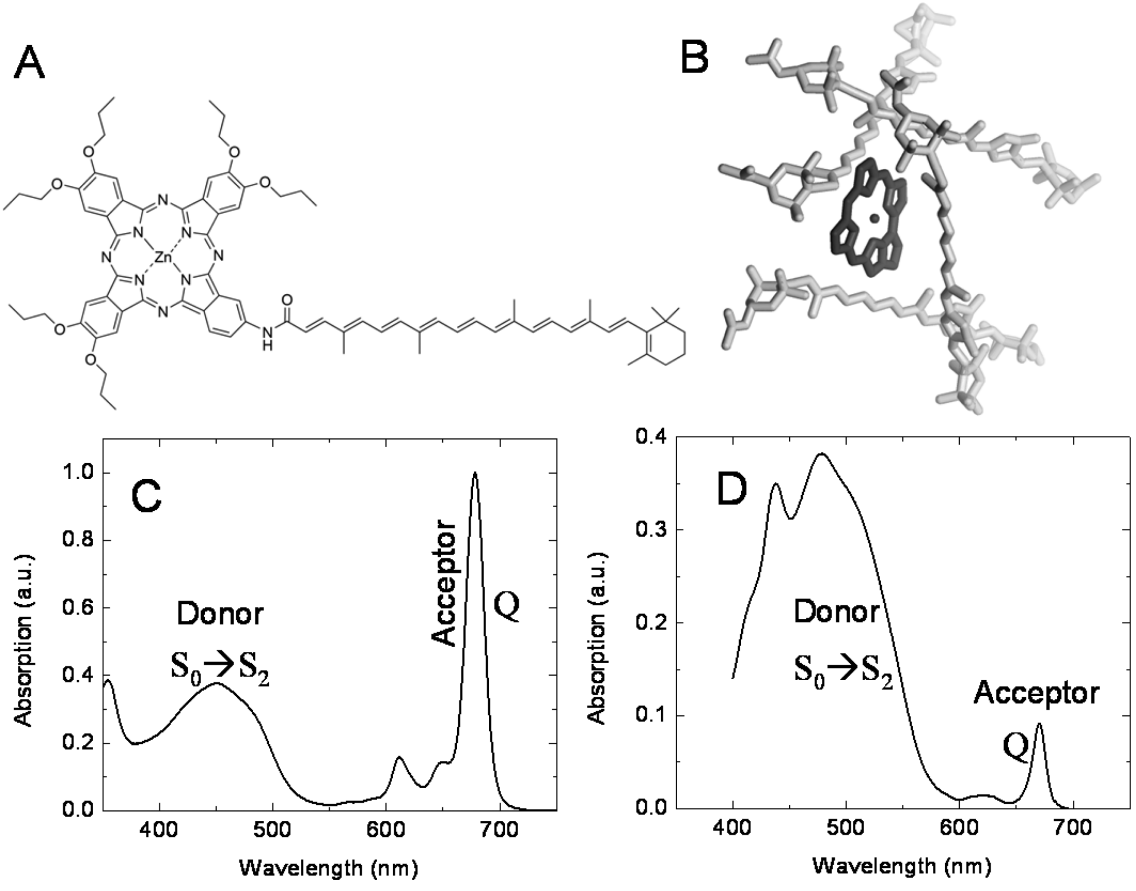

Figure 2. (A) The molecular structure of the caroteno-phthalocyanine dyad. (B) The crystal structure of a functional subunit of peridinin-chlorophyll protein. The structure has been rendered using the atomic coordinates determined by Hofmann et al.[27] (1ppr coordinate file form the RCSB Protein Data Bank) and the MOLMOL molecular graphics program.[28] The chlorophyll acceptor (dark gray) is surrounded by four peridinin donor molecules (light gray). (C) The absorption spectrum corresponding to the molecule in panel A dissolved in tetrahydrofuran. (D) The absorption spectrum of PCP.

dx.doi.org/10.1021/jp403301c | J. Phys. Chem. B 2013, 117, 11372−11382

Often many spectroscopic measurements including single-molecule and fluorescence imaging can only be performed practically in the annihilation regime. Therefore, it is important to know how the energy is transferred between two excited pigments to enable the correct interpretation of the measured data. To explore the differences between EET and annihilation rates, a transient ultrafast spectroscopic study was performed on two model carotenoid-containing systems for photosynthetic energy transfer: the first system is an artificially synthesized carotenoid-zinc-phthalocyanine dyade (CarZnPc) that has been designed as a model of an artificial light-harvesting antenna (Figure 2A), and the second system is a natural light-harvesting peridinin-chlorophyll protein (PCP) found in the dinoflagellate alga *Amphidinium carterae* (Figure 2B). Both systems have energy donor molecules (carotenoids) that absorb at shorter wavelengths than the acceptor pigments (phthalocyanine and chlorophyll *a* for the dyad and PCP, respectively). Due to the significant difference between the energies of the donor and acceptor excited states, the energy transfer in both systems is largely unidirectional and efficient with near-unity EET quantum yields.[17−21]

The prePump−Pump−Probe (pPPP) is a novel variant of the broadband incoherent multipulse spectroscopy that was formulated to simultaneously resolve EET and annihilation dynamics in molecular aggregate systems. Several modifications of this spectroscopy have been applied to unravel complex energy relaxation and transfer pathways in light-harvesting complexes[22,23] and photoreactive systems.[24−26] The approach used in this study involves three laser pulses (Figure 1B). The first (prePump) pulse excites the donor pigment, after which the excitation is allowed enough time to fully transfer to the acceptor. A second (Pump) pulse then excites the donor again, and the third broadband (Probe) pulse monitors the absorption changes in the sample. By varying the timing of the Probe pulse and alternating the presence of the prePump pulse, the prePump-induced differences in the Pump−Probe kinetics can be resolved.

2. EXPERIMENTAL SECTION

The CarZnPc dyad was synthesized as described previously[21] and was dissolved in THF at an optical density of 0.8/mm at the lowest energy absorption maximum (∼680 nm) (Figure 2C). The PCP was isolated and purified according to the procedure described earlier.[27] The optical density of the PCP sample was 0.5/mm at 475 nm. All measurements were performed in 1 mm optical path length quartz cuvettes at room temperature that were rapidly translated to ensure sample refreshment between consecutive laser shots. Comparison of the sample absorption spectrum before and after experiment showed that no significant photodamage of the sample occurred during the experiments.

The pump−dump−probe setup has been described in detail earlier[29,30] and has been modified to include a prePump pulse.[25] The basis of the system is a 1 kHz amplified Ti:sapphire system (BMI α−1000) delivering 400 μJ, 60 fs, 790 nm pulses. The dispersed pPPP experiments were performed at the Pump wavelengths of 475 nm for both CarZnPc and PCP samples. The prePump and Pump pulses were generated by a home-built noncollinear optical parametric amplifier (NOPA) pumped by the second harmonic (395 nm) of the fundamental. The white-light continuum, used as the broad-band probe pulse, was produced by focusing a weak 790 nm beam into a slowly translating CaF_2 crystal. The delays between prePump, Pump, and Probe pulses were varied via motorized, computer-controlled translation stages (Newport). The polarizations of the Pump and prePump pulses were set to the magic angle (54.7°) with respect to the Probe pulse. The prePump and Pump pulse intensities were between 200 and 400 nJ/pulse, and the beam waist at the sample was ∼300 μm in diameter. The prePump time was set to be 50 ps before the pump in both pPPP experiments discussed here.

Two mechanical choppers running at 150 and 300 Hz were used to sequentially block and unblock prePump and Pump beams, and the Probe spectra corresponding to different open/closed states of the choppers were synchronously binned. The Probe light spectra were recorded using a home-built double-diode array detector that allowed real-time shot-to-shot data acquisition.[29] The mechanical chopper status was determined by two photodiodes measuring the intensity of the prePump and Pump pulses. After the calculation of difference absorption, three data sets are obtained: Pump−Probe (PP) when the Pump pulse is on and the prePump pulse off, prePump−Probe (pPP) when the pump pulse is off and the prePump pulse on, and prePump−Pump−Probe (pPPP) when both prePump and Pump pulses are on. The collected data constitute three three-dimensional signals with 254 wavelength points and ca. 100 time points each. The wavelength resolution of the data is 1 nm with a ∼120 fs time resolution and an average noise level of ∼1 mOD. The group velocity dispersion (GVD) of the white light was estimated from the measurement of cross-phase modulation artifact in the solvent and was further refined in the global fitting procedure. All the data were corrected for GVD prior to presentation.

3. MODELING

The framework of analyzing the data of pPPP signals on the donor−acceptor aggregate systems studied here involves describing the populations of the electronic states of donors and acceptors as a function of time after excitation of the donor. To quantitatively describe the data, we consider two cases at t = 0: the acceptor is in its ground state (EET) or its excited state (annihilation). The model also has to provide the flexibility of making EET rates to an excited vs nonexcited acceptor different.

The complexity of the investigated systems is determined by two factors: (1) the excited state manifold of the donors and (2) the number of the donors and the acceptors within the system. The CarZnPc dyad has only one donor (carotenoid) and one acceptor (phthalocyanine) pigment (Figure 2A). However, the carotenoid has an optically one-photon forbidden S_1 state, which can be populated via internal conversion from the optically allowed S_2 and, in some cases, has been reported to donate singlet energy to the phthalocyanine.[31] The modeling is more complicated for PCP, since there are four donor molecules transferring energy to a single acceptor, chlorophyll *a* (Chl *a*), in the center of a monomer subunit (Figure 2B). The native form of monomeric PCP contains two such subunits that are nearly identical.[27] Upon excitation of peridinin, the excitation energy is rapidly (within a few ps) transferred to the Chl *a*.[32,33] After this, equilibration of energy between the Chl *a* molecules occurs on a ∼20 ps time scale and can thus be neglected when investigating peridinin-to-Chl *a* energy/annihilation kinetics studied here.[33] The excited state manifold of peridinin is even more complicated than that of "ordinary" carotenoids and involves an intramolecular charge transfer (ICT) state[34] that has energy similar to the S_1 state and

dx.doi.org/10.1021/jp403301c | J. Phys. Chem. B 2013, 117, 11372−11382

participates in the energy transfer process.[33] Since PCP is the more complicated of the two investigated systems, we first define our model for PCP and subsequently discuss the simplifications necessary to apply the same model to the CarZnPc dyad.

3.1. Monte Carlo Modeling. In small molecular aggregate systems, where the size of the aggregate is smaller or comparable to the excitation diffusion radius, both EET and the annihilation dynamics are well described with the deterministic population flow model based on Master equation approaches.[3,11] However, in our case, where the donor molecules have more than one excited state participating in the EET, *and* the EET rate may differ from the annihilation rate (in principle), this approach is unusable. To follow the details of the EET and annihilation, it is more convenient to employ a Monte Carlo (MC) approach, akin to that presented by Demidov,[35] where all the processes, both linear and nonlinear, that affect population dynamics in the system can be explicitly coded.

We start by defining the energy migration model for PCP, which is based on the EET scheme depicted in Figure 3. The

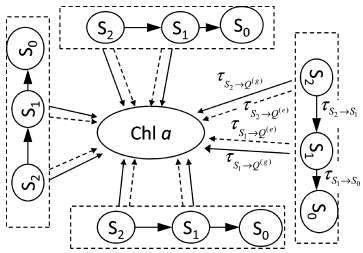

Figure 3. Schematic representation of the model for population dynamics in a functional unit of PCP. The peridinins are modeled with two excited states each, both contributing to the energy transfer. The solid arrows represent the transfer to the Chl *a* in the ground state, the dashed ones in the excited state. Internal conversion in the peridinins is also included. The notation of the corresponding rate constants is shown next to the respective arrows.

peridinin molecules are represented with two excited states (S_2 and S_1) capable of energy transfer with time constants $\tau_{S_2\to Q^{(g)}}$, $\tau_{S_1\to Q^{(g)}}$ and $\tau_{S_2\to Q^{(e)}}$, $\tau_{S_1\to Q^{(g)}}$ to the nonexcited and excited acceptor, respectively. These two states are also connected to each other via internal conversion (time constant $\tau_{S_2\to S_1}$). The S_1 state can either transfer excitation energy directly to the Chl *a* or decay to the ground state (time constant $\tau_{S_1\to S_0}$). The "hot" S_1 and the ICT populations that are also observed in peridinin and PCP[33,36] are neglected for the sake of simplicity. However, the modifications necessary to expand the model to account for these states are straightforward.

Each realization starts with a certain number of excitations placed in the peridinin S_2 state, because it is the only state that can be accessed by the optical excitation.[37] The initial number of excitations is a random number obeying the binomial distribution with the mean number of excitations ξ_{PP} corresponding to the experimental excitation conditions (reflecting the intensity of the pump pulse). The initial conditions are registered as the state of the system at time zero. The time step was selected to be sufficiently small such that the probability for an excitation to hop twice is negligible and an excitation on the *i*th compartment in Figure 3 can hop to one of the neighboring compartments. This probability of transfer to every neighbor is proportional to the respective energy transfer (or internal conversion) rate. The probability $g_{ii}(t)$ for the excitation on the same *i*th site to remain in its original position is described by the following differential equation:

$$\frac{dg_{ii}(t)}{dt} = -\left(\sum_j k_{i\to j}\right) g_{ii}(t) \tag{2}$$

where $k_{i\to j} \equiv 1/\tau_{i\to j}$ is the excitation energy transfer (or internal conversion) rate from the *i*th to *j*th compartment (see Figure 3 for the possibilities of what *i* and *j* can stand for).

At $t = 0$, the excitations are in their original positions (i.e., $g_{ii}(0) = 1$), and the integration of eq 2 yields

$$g_{ii}(t) = e^{-(\sum_j k_{i\to j})t} \tag{3}$$

In the scheme (Figure 3), the probability of finding the excitation in the *m*th compartment is

$$g_{im}(t) = \frac{k_{i\to m}}{\sum_j k_{i\to j}}\left(1 - e^{-(\sum_j k_{i\to j})t}\right) \tag{4}$$

where $i \neq m$. Equations 3 and 4 express the fact that during a time period an excitation can either hop to one of the neighboring compartments (i.e., via EET or internal conversion) or remain in its original position (i.e., $g_{ii}(t) + \sum_m g_{im}(t) = 1$). Thus, at every time step in the Monte Carlo realization, for each excitation in the structure, a random number between 0 and 1 is generated. This interval is divided into sections according to the probabilities given by eqs 3 and 4 and, depending on which section the generated number falls into, a "target" is determined; i.e., the compartment is found where the excitation will go after the time period *t*. Note that eqs 3 and 4 become meaningless at longer times, when the probability of the excitation to be transferred twice becomes considerable. Hence, the time step *t* was selected to be chosen such that

$$\left(1 - e^{-(\sum_j k_{i\to j})t}\right)^2 \approx 0 \tag{5}$$

which is typically ~5% of the fastest EET rate observed.

One reason for limiting the time step is that when the first excitation is transferred to Chl *a* (Figure 3), the EET rates change (since the acceptor becomes excited, $\tau_{S_2\to Q_y^{(e)}}$ and $\tau_{S_1\to Q_y^{(e)}}$ are used instead of $\tau_{S_2\to Q_y^{(g)}}$ and $\tau_{S_1\to Q_y^{(g)}}$, respectively) and the probabilities given by eqs 3 and 4 have to be recalculated. A second reason is that eqs 3 and 4 describe only single excitation dynamics with no annihilation. This is accounted for "between" the time steps: if an acceptor is excited, and the donor excitation has to go there, the donor excitation effectively "disappears". If, however, the target (acceptor) compartment is not excited, and the excitation on the donor "decides" to go there, the excitation on the donor disappears and the acceptor becomes excited.

This time stepping procedure is repeated until the dynamics is obtained in a desired time window. The dynamics is then averaged from a large number (typically ca. 10 000) of realizations to obtain a statistically meaningful result with a desired signal-to-noise ratio.

3.2. Calculation of prePump–Pump–Probe Data. To compare the results of the Monte Carlo modeling with the experiment, the signals measured in a pPPP experiment have to be explicitly calculated. For that, we have to describe three signals: PP, pPP, and pPPP. The PP dynamics is described by

dx.doi.org/10.1021/jp403301c | J. Phys. Chem. B 2013, 117, 11372–11382

the populations $n_i^{(PP)}$ of the different compartments (Figure 3), that are obtained directly from the Monte Carlo model described above. For the pPPP signals, the modeling has to be repeated with a different initial condition with an excitation present on Chl *a* at $t = 0$. Hence, in this case, only the energy transfer time constants pertaining to the excited acceptor $\tau_{S_2 \to Q_y^{(e)}}$ and $\tau_{S_1 \to Q_y^{(e)}}$ are used. If the fraction of Chl *a* molecules excited by the prePump pulse is p, the population dynamics in pPPP data is described by

$$n_i^{(pPPP)}(t) = p n_i^{(ex)}(t) + (1 - p) n_i^{PP}(t) \tag{6}$$

where $n_i^{(pPPP)}(t)$ are the populations of different compartments in the pPPP data and $n_i^{(ex)}(t)$ are the populations calculated with the initial condition, when then Chl *a* is excited at $t = 0$. In the pPP data set, the excitations are equilibrated on the acceptor and the populations of different compartments are constant: $n_i^{(pPPP)}(t) = 0$, when the value of i corresponds to the states S_1, S_2, and $n_i^{(ex)}(t) = p$, when the value of i corresponds to Chl *a*.

The calculated populations $n_i^{(PP)}$, $n_i^{(ex)}(t)$, and $n_i^{(pPPP)}(t)$ of different compartments are convoluted with an instrument response function (IRF):

$$m(t) = \int_{-\infty}^{+\infty} n(\tau) \mathrm{IRF}(t - \tau)\, \mathrm{d}\tau \tag{7}$$

(the indices of the populations are omitted here). The measured pPPP signals of experiments presented here can be well described with a Gaussian IRF with the full width at half-maximum of 120 fs. Finally, the wavelength-dependent amplitudes $\sigma_i(\lambda)$ of different compartments are calculated and the final model functions that can be directly compared with the data are

$$\begin{aligned} \mathrm{PP}(t, \lambda) &= \sum_i m_i^{(PP)}(t)\sigma_i(\lambda) \\ \mathrm{pPP}(t, \lambda) &= \sum_i m_i^{(PrP)}(t)\sigma_i(\lambda) \\ \mathrm{pPPP}(t, \lambda) &= \sum_i m_i^{(PrPP)}(t)\sigma_i(\lambda) \end{aligned} \tag{8}$$

The wavelength dependent amplitudes of the different compartments $\sigma_i(\lambda)$, also referred to as species-associated difference spectra (SADS), are linear parameters of the model and can be estimated via linear regression and solving the normal equations by singular value decomposition.[38] In this respect, the modeling presented here is just another form of global or target analysis,[39,40] with the difference that the Monte Carlo method is used to estimate the concentrations of the different compartments instead of solving a system of linear differential equations (which cannot be applied for the analysis of excitation annihilation because the latter is inherently a nonlinear process involving two or more excitations).[3]

3.3. Modifications of the Model to Describe the CarZnPc Dyad. The model can be easily adjusted to describe the data measured on the CarZnPc dyad. For CarZnPc, only one out of four carotenoids shown in Figure 3 is included in the model. This special case is also useful because the system is significantly simpler with a single donor and a single acceptor and the excitation dynamics can be described using the following set of kinetic equations:

$$\begin{aligned} \frac{\mathrm{d}n_{S_2}}{\mathrm{d}t} &= I(t) - \frac{1}{\tau_{S_2 \to Q}} n_{S_2} - \frac{1}{\tau_{S_2 \to S_1}} n_{S_2} \\ \frac{\mathrm{d}n_{S_1}}{\mathrm{d}t} &= \frac{1}{\tau_{S_2 \to S_1}} n_{S_2} - \frac{1}{\tau_{S_1 \to Q}} n_{S_1} - \frac{1}{\tau_{S_1 \to S_0}} n_{S_1} \\ \frac{\mathrm{d}n_{Q_y}}{\mathrm{d}t} &= \frac{1}{\tau_{S_2 \to Q}} n_{S_2} - \frac{1}{\tau_{S_1 \to Q}} n_{S_1} \end{aligned} \tag{9}$$

Here, n_i represent the populations of different compartments and the rate constants τ_i are different depending on which initial condition is used (with or without prePump of the acceptor). Note that such a description using differential equations is only possible in a single donor–acceptor pair, where only one energy transfer event can occur and there is no complication of having to recalculate the rates for excited acceptor. The calculations using eq 9 were performed, and the results were identical to those yielded by the Monte Carlo model (not shown).

4. RESULTS

4.1. Energy Transfer Dynamics Observed by Pump–Probe Signals. The EET dynamics in both systems is evident from the dispersed PP data (Figure 4). Similar experiments on

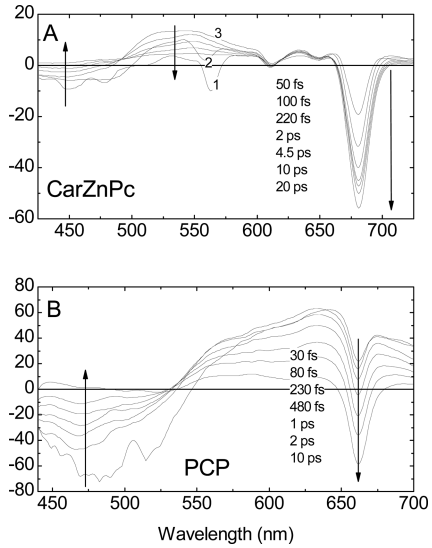

Figure 4. Time-gated PP spectra measured at different delay times for the CarZnPc dyad (A) and PCP (B). In panel A, the first three spectra have been labeled, whereas the others follow the trend indicated by the arrows. The probe delay times are indicated in the legends.

PCP have been performed before, and the energy transfer rates and pathways have been presented.[20,33] Detailed analysis of the EET time scales in the CarZnPc dyad was also presented elsewhere;[41] here we will briefly summarize the observed spectroscopic features of EET in both systems, before delving into the analysis of the more complex pPPP data.

The dispersion-corrected PP spectra measured at different probe delay times for both investigated systems are shown in Figure 4. EET manifests itself as the decay of the characteristic spectrum of Car* with concomitant growth of the Pc* spectrum or Chla* for the CarZnPc and PCP systems, respectively. In the CarZnPc dyad (Figure 4A) that has an overall EET yield of ca. 90%,[41] the ground state bleach (GSB)

dx.doi.org/10.1021/jp403301c | J. Phys. Chem. B 2013, 117, 11372–11382

and stimulated emission (SE) band of the phthalocyanine (a sharp negative band around 680 nm, see also Figure 2) is observed already in the 50 fs spectrum, indicating that a significant part of EET proceeds from the short-lived S_2 state. This spectrum also exhibits a negative artifact at 560 nm (due to stimulated Raman scattering) of the pump light in the solvent and a broader negative feature around 480 nm due to the SE from the S_2 state of the carotenoid. Below 480 nm, a GSB band of the carotenoids is observed (Figure 2). In the later spectra, a part of the carotenoid GSB is still observed along with a new positive band around 540 nm due to the $S_1 \rightarrow S_n$ excited state absorption (ESA).[37] As these bands decay, further growth is observed in the phthalocyanine region, indicating that the S_1 state also contributes to the energy transfer. The "terminal" spectrum is reached after ca. 20 ps, which exhibits no further spectral evolution and decays on an ~3 ns time scale. This spectrum is entirely due to the excited state of the phthalocyanine (Pc*) and is characterized by the GSB and SE band around 680 nm which is superimposed on the broad featureless ESA band with a maximum around 550 nm. Several dips (650 nm, 610 nm) follow the absorption spectrum due to the bleach of vibronic sub-bands of Q_y and the Q_x transition of the phthalocyanine (Figure 2).

Energy transfer in PCP has been well investigated by Frank, van Grondelle, Sundström, and others; an overall energy transfer efficiency of ca. 88% has been reported,[19] and several time scales have been found.[20,32,33,42−45] As with the CarZnPc dyad signals, the 30 fs PP spectrum (Figure 4C) already exhibits a dip around 660 nm, which is due to the GSB/SE of the Chl *a*. At the same time, a negative feature due to the GSB (and SE from the S_2 state) of peridinin (Car*) is observed at wavelengths between 440 and 550 nm. The fast decay of this spectrum indicates that a significant portion of energy transfer proceeds through S_2 with a 100 fs lifetime.[32,33] Later, the S_1/ICT state is formed that features the carotenoid GSB at ca. 470 nm and a pronounced ESA band between 530 and 700 nm. As this feature decays on the time scale of several picoseconds, a further growth of the Chl *a* GSB/SE band is observed, indicating that S_1/ICT states also donate energy to the Chl *a* in PCP.

4.2. Annihilation Dynamics Observed in prePump−Pump−Probe Signals. In the absence of annihilation dynamics, the difference absorption induced in the sample, by both prePump and Pump pulses, is equal to the sum of difference absorptions induced by each of the pulses separately. An example of such a situation is the limiting case, when the prePump and Pump pulses are very weak or when prePump and Pump pulses access different subpopulations of the donor molecules:

$$\Delta\Delta\mathrm{OD}(t, \lambda) \equiv \mathrm{PrPP}(t, \lambda) - \mathrm{PrP}(t, \lambda) - \mathrm{PP}(t, \lambda) = 0$$

This is a noninformative measurement (at least beyond PP signals alone). However, when excitations do annihilate, the observed effect should be that the $\mathrm{pPPP}(t, \lambda)$ signal at the acceptor wavelengths is smaller in its absolute value than the sum of $\mathrm{pPP}(t, \lambda)$ and $\mathrm{PP}(t, \lambda)$ signals: some excitations annihilate on the acceptors, and the resulting amount of excited acceptors is decreased. This effect is evident in Figure 5, where the $\mathrm{pPPP}(t, \lambda)$ spectra are compared to the sum of $\mathrm{pPP}(t, \lambda)$ and $\mathrm{PP}(t, \lambda)$ spectra for both systems at the time when the energy transfer is completed (20 ps for the CarZnPc dyad and 10 ps for PCP). The $\Delta\Delta\mathrm{OD}(t, \lambda)$ spectrum is identical to the inverted acceptor spectrum (compare with the corresponding

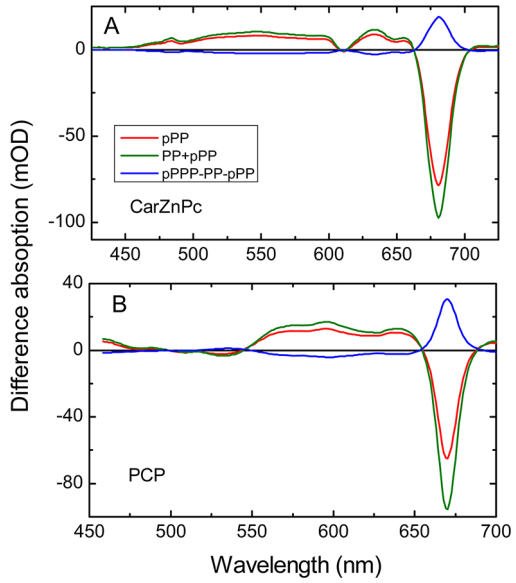

Figure 5. pPPP (red lines), the sum of PP and PrP (green lines), and pPPP-PP-PrP (blue lines) spectra measured on CarZnPc dyad (A) and PCP (B). The probe delay was 20 ps for parts A and B and 10 ps for part C.

late PP spectra in Figure 4), which indicates the loss of the acceptors (Pc* or Chla*) due to annihilation. Note that this difference cannot be due to the removal of population from the ground state of the donor, important when the prePump and Pump pulses arrive almost simultaneously:[22] at the time when the second excitation pulse arrives, all the excitations have reached the acceptor molecules and the carotenoids are back to their ground states. From the amount of the loss, the amount of the acceptor population lost due to annihilation can be estimated to be between 15 and 33%, depending on the system.

4.2.1. CarZnPc Dyad. The pPPP results on the CarZnPc dyad are shown in Figure 6. The filled squares show the PP data (the spectra representing the same data are shown in Figure 4A), the open circles represent the pPPP data (both prePump and Pump pulses present), and the solid triangles show the pPP data (prePump pulse present, Pump pulse absent). In the PP data at 440 nm (Figure 6A), the wavelength corresponding to the GSB of carotenoid, two decay time scales are observed. The first is of the order of 100 fs and corresponds to the loss of carotenoid excited states due to the EET from S_2. The second time scale can be attributed to the loss of the carotenoid S_1 state due to EET and/or internal conversion. At 495 nm (Figure 6B), early pump probe signals are dominated by the SE from the carotenoid S_2 state, whereas at later times the positive ESA from the S_1-to-S_n transition of the carotenoid starts to dominate and decays with the same rate as the trace measured in the carotenoid GSB region (440 nm). A relatively "clean" (i.e., uncluttered by the overlap with the difference absorption bands due to S_2 and the phthalocyanine) carotenoid S_1 signal is observed at 537 nm (Figure 6C, filled squares), where a near-instantaneous rise is observed as the internal conversion from S_2 to S_1 occurs and is followed by a several picosecond decay as the S_1 energy is transferred to the phthalocyanine and/or relaxes to the ground state of carotenoid. The GSB and SE kinetics of the phthalocyanine acceptor is best observed at 682 nm (Figure 6D), where the trace exhibits a biphasic growth, one phase being near-instantaneous and corresponding to the EET from the carotenoid S_2 state and another phase with a

dx.doi.org/10.1021/jp403301c | J. Phys. Chem. B 2013, 117, 11372−11382

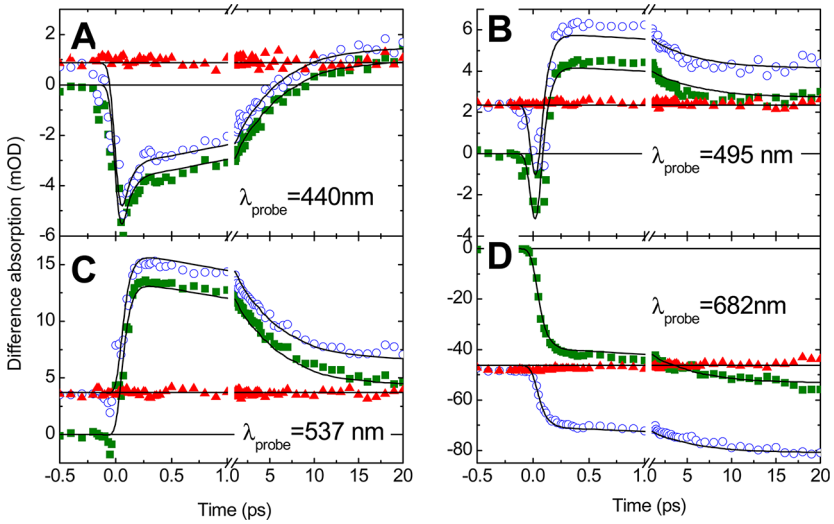

Figure 6. Pump−probe (green squares), prePump−Probe (red triangles), and prePump−Pump−Probe (blue circles) traces measured on the CarZnPc dyad in THF at different characteristic probe wavelengths. The probe wavelengths are indicated on the graphs. The prePump time was 50 ps before the pump pulse. Solid lines show a global fit to the data based on the Monte Carlo model. The parameters of the fit are given in Table 1. Note the break in the time axis at 1 ps.

characteristic time of ca. 10 ps corresponding to the EET from the carotenoid S_1 state. By comparing the amplitudes of both phases, we conclude that ca. 75% of the total EET in this dyad proceeds via S_2.

The filled triangles in Figure 6 represent the pPP signals with the prePump set at 50 ps before the pump pulse, and hence, the signals shown in the graph correspond to PP signals in the time window from 50 to 70 ps. As expected, the data are essentially time-independent and the amplitudes of the traces follow the spectrum of excited phthalocyanine (compare with the 20 ps spectrum in Figure 4A).

The pPPP data at 682 nm correspond to the GSB/SE band of the phthalocyanine (open circles in Figure 6D) and indicate clearly that a significant portion of excitations annihilate after prePump (i.e., the subpopulations of the sample accessed by the prePump and Pump pulses overlap to a significant extent): the Pump pulse in a PP experiment results in the terminal phthalocyanine GSB signal of 56 mOD (filled squares in Figure 6D), whereas the same pulse applied *after the prePump* increases the bleach from ca. 48 mOD (initial value of open circles) to 80 mOD (terminal value), i.e., by only 32 mOD. Interestingly enough, *no* significant differences in the PP vs pPPP kinetics are observed at the carotenoid-characteristic wavelengths (Figure 6A−C), apart from the offset resulting from the prePump-induced difference spectrum due to the excited acceptor. These kinetics directly reflect the decay of the donor signal, and their difference would indicate the different EET rate caused by the excitation residing on the acceptor.

To summarize, in the CarZnPc, the EET rate is approximately the same regardless of the electronic state of the phthalocyanine acceptor. This observation is further confirmed by the Monte Carlo modeling, where the same energy transfer rates for excited and nonexcited acceptor ($\tau_{S_2\rightarrow Q^{(e)}} = \tau_{S_2\rightarrow Q^{(g)}}$ and $\tau_{S_1\rightarrow Q^{(e)}} = \tau_{S_1\rightarrow Q^{(g)}}$, Figure 3) have been used to produce a satisfactory fit to the data shown by the solid lines in Figure 6 (the estimated parameters are summarized in Table 1).

The SADS estimate from the Monte Carlo fit to the data (Figure 7A) provides further credence to the validity of the model, since they agree with previously reported SADS.[20,21] The SADS obtained for S_2 (solid line) features pronounced S_2 SE at the wavelengths between 500 and 575 nm with an intense negative peak at 565 nm that is ascribed to the stimulated Raman scattering in the solvent. This SADS also shows some feature in the phthalocyanine absorption region (around 680 nm) that is similar to the second derivative (narrowing) of the band at 680 nm. This could be an electrochromic "Stark" effect due to the interaction between the dipole moment of the carotenoid S_2 state and the phthalocyanine molecule.[46] The S_1 SADS (green line in Figure 7) exhibits a typical ESA band[37] around 570 nm and the carotenoid GSB below 500 nm. Finally, the SADS of the excited phthalocyanine molecule (dotted line in Figure 7) is identical to the 20 ps pump−probe spectrum (Figure 4A).

Table 1. Parameters Estimated from Fitting the Monte Carlo Model to the pPPP Data

parameter/system	CarZnPc dyad	PCP
$\tau_{S_2\rightarrow S_1}$	200 fs	75 fs
$\tau_{S_1\rightarrow S_0}$	14 ps	12 ps
$\tau_{S_2\rightarrow Q_y^{(g)}}$	75 fs	150 fs
$\tau_{S_2\rightarrow Q_y^{(e)}}$	75 fs	150 fs
$\tau_{S_1\rightarrow Q_y^{(g)}}$	8 ps	2 ps
$\tau_{S_1\rightarrow Q_y^{(e)}}$	8 ps	2 ps
ξ_{PP}	0.45	1.25
p	0.35	0.45

4.2.2. Peridinin-Chlorophyll Protein. In PCP, the general picture is similar to CarZnPc, except no clear spectral region exists where the acceptor (Chl *a**) population could be observed uncluttered by the transient absorption bands of peridinin (Car*). The pPPP traces at different probe wavelengths are shown in Figure 8. Following the same logic as with the previous system, the comparison of the terminal signals at the Chl *a* characteristic wavelength (662 nm, Figure 8D) verifies that annihilation does occur in the pPPP experiment: the pump-induced absorption difference at 10 ps delay is −58 mOD in the absence, while the presence of the

dx.doi.org/10.1021/jp403301c | J. Phys. Chem. B 2013, 117, 11372−11382

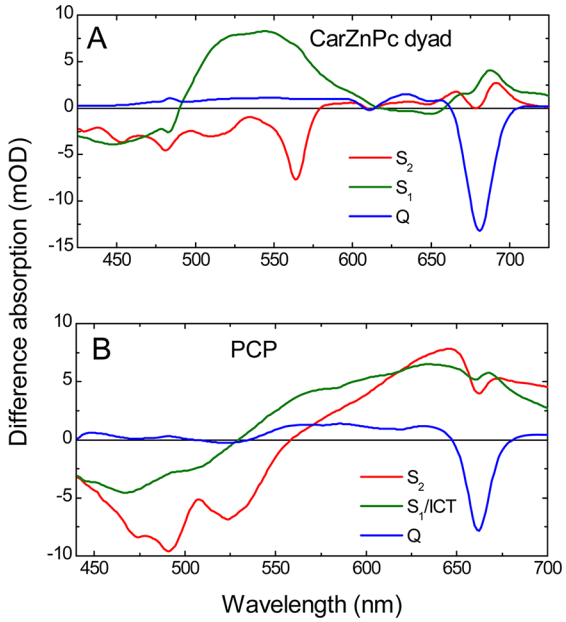

Figure 7. Species associated difference spectra of the CarZnPc dyad (A) and PCP (B), resulting from the fits of the Monte Carlo model to the data. S_1, S_1/ICT, and S_2 denote the excited states of carotenoids, and Q stands for the lowest excited state of phthalocyanine and Chl *a*. The estimated rates corresponding to the arrows in Figure 3 are given in Table 1.

prePump (which on its own right induces −35 mOD of bleach signal) results in the addition of only −8 mOD. Therefore, the combined effect of prePump and Pump is just −66 mOD instead of −92 mOD that would be observed in the case of no annihilation. Again, little to no difference is induced by the prePump on the decay kinetics of the donors, which can be clearly observed in the kinetic traces measured at the wavelengths corresponding to the GSB (Figure 8A), SE from S_2 (Figure 8B), and ESA of S_1/ICT (Figure 8C) states of peridinin. Here, the signals contain only the contribution from peridinins, and the pPPP signal is virtually identical to the PP signal, indicating that, although some of the complexes have their Chl *a* pigments in the excited state, the EET rate remains unchanged.

This is confirmed by the Monte Carlo model that allows us to estimate the average number of excitations per complex (Table 1) and estimates the SADS (Figure 7C) that coincide closely with the spectra reported previously.[32] The estimated EET time constants also agree well those previously reported.[32,33] The S_2 SADS features a broad SE band extending from 475 to 560 nm and S_2-to-S_n ESA at the wavelengths longer than 560 nm. In the SADS of S_1/ICT, the SE is absent and only the GSB of peridinin remains, resulting in a negative difference absorption below 525 nm. A broad ESA band due to the S_1-to-S_n transition (blue-shifted compared to the ESA of S_2) is observed above 525 nm, and peaks at around 640 nm. Finally, the SADS of the excited Chl *a* shows a negative GSB/SE band peaking at ca. 670 nm and a relatively flat ESA over the region between 540 and 650 nm, which is virtually the same as the spectrum of excited Chl *a* in solution.[47]

5. DISCUSSION

In both the investigated PCP and dyad systems, the energy transfer kinetics are largely independent of whether the acceptor molecules are excited or not, even though the excitation annihilation process has clearly been observed in both pPPP experiments. This finding has been reconfirmed by the Monte Carlo modeling that produced a satisfactory fit to the data (Figures 6 and 8) and provided the SADS matching our *a priori* knowledge about the investigated light-harvesting systems, while using the same EET rate for the excited and ground state acceptor.

The fits shown in Figures 6 and 8 do show some systematic errors. However, these are probably due to the simplifications used in the modeling, rather than the failure to fit the data with *identical* EET and annihilation rates. Several aspects have been left out of the model, and implementing those might improve the quality of the fits. First, we have assumed that the energy transfer occurs with one single rate, thereby neglecting any structural or spectral heterogeneity that is always present in the light-harvesting complexes.[48] Such heterogeneity results in a distribution of EET rates within the sample, and multi-

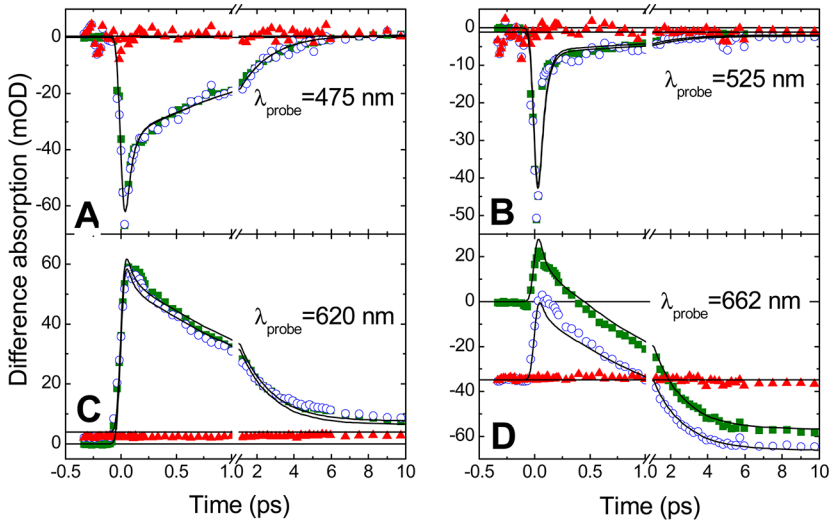

Figure 8. Pump−probe (filled squares), prePump−probe (filled triangles), and prePump−pump−probe (open circles) traces measured on PCP at four characteristic probe wavelengths (indicated on the graphs). The prePump time was 50 ps before the Pump. The solid lines show a global fit to the data based on the Monte Carlo model. The parameters of the fit are given in Table 1.

dx.doi.org/10.1021/jp403301c | J. Phys. Chem. B 2013, 117, 11372−11382

exponential EET kinetics is observed. The multiexponential kinetics may partly account for the discrepancies between the data and the modeling. Second, the model implicitly assumes that the observed dynamics is entirely due to the population transfer between the discrete electronic states (S_1, S_2, Q) that feature specific spectra. Thus, processes like solvation and vibrational relaxation that result in continuous spectral dynamics like shifting and/or narrowing[49−51] are not included in our model. Although solvation is assumed to be near-instantaneous (<100 fs) in proteins,[52] in artificial light-harvesting systems dissolved in organic solvents, solvation and vibrational cooling can certainly affect the observed picosecond PP and pPPP dynamics.[53] Usually, solvation and vibrational relaxation can be fitted using compartmental models that include extra compartments that do not represent separate electronic states but rather represent the spectral changes due to these processes.[40] To keep the description model simple, such compartments were not included in the presented model; doing so may result in a better agreement between modeled and measured data. Third, while analyzing the data on the systems having carotenoids as the light-harvesting pigments, it is important to remember that the excited-state manifold of carotenoids is much more complex than our model suggests.[37] In particular, in light-harvesting carotenoids in solution and inside the protein, a sub-ps relaxation process has been observed and ascribed to a vibrationally hot S_1 state,[54] which also acts as an energy donor adding further complexity to the system. In PCP, the EET pertaining to the S_1/ICT manifold has been found to be multiexponential with 700 fs and 2.5 ps lifetimes,[33] whereas here it was modeled with a single lifetime of 2 ps and thus some part of the dynamics could not be precisely reproduced.

Addressing the aforementioned issues in the model would result in better fits to the data in Figures 6 and 8. However, the focus here is not on describing the EET dynamics but rather the *differences in EET* induced by the pre-excitation of the system. In this respect, the model provides an adequate description of the experimental observations, and the qualitative conclusions are already evident from the raw data: the EET rate is largely independent of the acceptor state (ground vs excited state).

Interpreting this finding in terms of the Förster EET model (eq 1), the results would imply that the separations and directions of the transition dipole moments for S_1-to-S_n and S_0-to-S_1 transitions are approximately equal for the two transitions, as are the spectral overlaps between the S_0-to-S_1 absorption and S_1-to-S_n. A pathological case where a change in the direction (or magnitude) of the dipole moment would be compensated by a change in the spectral overlap can be excluded on the basis of two systems studied: it is unlikely that the same coincidence occurs in both of them. The directions of the transition dipoles are largely defined by the spatial structure and orientation of the pigment; for example, in the carotenoids, it always lies more or less along the direction of the backbone of the molecule.[4] Thus, it is natural to expect that in many cases the transition moment of S_1-to-S_n transition will be parallel (or, rather, approximately parallel) to that of S_0-to-S_1, especially since S_n is not one state but a manifold of excited states above S_1, some of which will have their transition dipoles parallel to the one of the S_0-to-S_1 transition. The equality of spectral overlaps is more difficult to address; however, for chlorophyll pigments, they have been calculated to be similar.[55] The molecular absorption and fluorescence spectra are quite broad at room temperature and feature a number of vibronic sub-bands at the energies above the lowest transition. Due to the large width of the spectra, the spectral overlap is often not a critical parameter for EET and it might not affect the EET rate significantly when the state of the acceptor changes. It is important to note that the Förster EET model assumes the relaxed excited state of the donor,[15] which—at least in the case of the carotenoid S_2 state—is debatable, and hence the attempts to interpret the EET rates based on dipole moment orientations and spectral overlaps may be too simplistic. However, the conclusion of the equality of the EET rates is drawn purely from the experimental observations and is independent of the specific model of EET.

On the basis of the example of only two investigated light-harvesting systems, it would, of course, be too general to suggest that the EET rate is always equal to the annihilation rate in all photosynthetic systems. In fact, to provide further credence to the findings about the carotenoid-porphyrin systems investigated in this study, an additional experiment with direct pre-excitation of the acceptor (instead of pre-excitation of the donor followed by the energy transfer to the acceptor) would have to be performed. However, the application of the three-pulse pPPP approach is a straightforward and efficient method to resolve these differences. In combination with the presented Monte Carlo modeling, it can also give quantitative estimates of the corresponding EET rates.

6. CONCLUDING COMMENTS

A novel three-pulse femtosecond prePump−Pump−Probe experiment was used to characterize the differences in primary step in energy transfer and annihilation dynamics in two light-harvesting systems: the synthetic CarZnPc dyad and the natural pigment−protein complex PCP of *Amphidinium carterae*. No differences between EET and annihilation rates were observed in either of the systems, which suggests that the acceptor properties in these systems (orientation of the transition dipole moments and the overlap of the absorption spectrum with the donor) do not change significantly upon excitation. Such findings are unexpected and merit a further, more detailed study.

AUTHOR INFORMATION

Notes

The authors declare no competing financial interest.

ACKNOWLEDGMENTS

We would like to thank Professor Roger Hiller from the School of Biological Sciences, Macquarie University, Australi,a for supplying the PCP samples. M.V. was supported by The Netherlands Organization of Fundamental Research of Matter (FOM) and European Community's social foundation under Grant Agreement No. VP1-3.1-ŠMM-08-K-01-004/KS-120000-1756. D.S.L. is grateful to the Human Frontier Science Program Organization for providing financial support with a Career Development Award (CDA0016/2007-C).

REFERENCES

(1) Agranovich, V. M.; Galanin, M. D. *Electronic Excitation Energy Transfer in Condensed Matter*; North-Holland Publishing Company: Amsterdam, New York, Oxford, 1982.

(2) Pope, M.; Swenberg, C. E. *Electronic Processes in Organic Crystals and Polymers*; Oxford University Press: New York, 1999.

(3) Valkunas, L.; Trinkunas, G.; Liuolia, V. Exciton Annihilation in Molecular Aggregates. In *Resonance Energy Transfer*; Andrews, D. L.,

Demidov, A. A., Eds.; J. Wiley and Sons: Chichester, U.K., 1999; pp 244−307.
(4) van Amerongen, H.; Valkunas, L.; van Grondelle, R. *Photosynthetic Excitons*; World Scientific: Singapore, 2000.
(5) Psencik, J.; Ma, Y. Z.; Arellano, J. B.; Hala, J.; Gillbro, T. Excitation Energy Transfer Dynamics and Excited-State Structure in Chlorosomes of Chlorobium Phaeobacteroides. *Biophys. J.* **2003**, *84*, 1161−1179.
(6) Miller, M.; Cox, R. P.; Gillbro, T. Energy-Transfer Kinetics in Chlorosomes from Chloroflexus-Aurantiacus - Studies Using Picosecond Absorbency Spectroscopy. *Biochim. Biophys. Acta* **1991**, *1057*, 187−194.
(7) Larsen, J.; Bruggemann, B.; Polivka, T.; Sundstrom, V.; Akesson, E.; Sly, J.; Crossley, M. J. Energy Transfer within Zn-Porphyrin Dendrimers: Study of the Singlet-Singlet Annihilation Kinetics. *J. Phys. Chem. A* **2005**, *109*, 10654−10662.
(8) Trinkunas, G. Probing of Molecular Aggregates with Exciton Annihilation. *J. Lumin.* **2003**, *102*, 532−535.
(9) Gulbinas, V.; Jakubenas, R.; Pakalnis, S.; Undzenas, A. Dynamics of Charge Carrier Precursor Photogeneration in Titanyl Phthalocyanine. *J. Chem. Phys.* **1997**, *107*, 4927−4933.
(10) Valkunas, L.; Gulbinas, V. Nonlinear Exciton Annihilation and Local Heating Effects in Photosynthetic Antenna Systems. *Photochem. Photobiol.* **1997**, *66*, 628−634.
(11) Barzda, V.; Gulbinas, V.; Kananavicius, R.; Cervinskas, V.; van Amerongen, H.; van Grondelle, R.; Valkunas, L. Singlet-Singlet Annihilation Kinetics in Aggregates and Trimers of Lhcii. *Biophys. J.* **2001**, *80*, 2409−2421.
(12) Trinkunas, G.; Herek, J. L.; Polivka, T.; Sundstrom, V.; Pullerits, T. Exciton Delocalization Probed by Excitation Annihilation in the Light-Harvesting Antenna Lh2. *Phys. Rev. Lett.* **2001**, *86*, 4167−4170.
(13) Ovchinikov, A. A.; Timashev, S. F.; Belyi, A. A. *Kinetics of Diffusion-Controlled Chemical Processes*; Nova: New York, 1989.
(14) Hofkens, J.; Cotlet, M.; Vosch, T.; Tinnefeld, P.; Weston, K. D.; Ego, C.; Grimsdale, A.; Mullen, K.; Beljonne, D.; Bredas, J. L.; et al. Revealing Competitive Forster-Type Resonance Energy-Transfer Pathways in Single Bichromophoric Molecules. *Proc. Natl. Acad. Sci. U.S.A.* **2003**, *100*, 13146−13151.
(15) Förster, T. Delocalized Excitation and Excitation Transfer. In *Modern Quantum Chemistry*; Sinanoglu, O., Ed.; Academic Press: New York, 1965; Vol. *IIIB*, pp 93−137.
(16) Cotlet, M.; Gronheid, R.; Habuchi, S.; Stefan, A.; Barbafina, A.; Mullen, K.; Hofkens, J.; De Schryver, F. C. Intramolecular Directional Forster Resonance Energy Transfer at the Single-Molecule Level in a Dendritic System. *J. Am. Chem. Soc.* **2003**, *125*, 13609−13617.
(17) Pillai, S.; Ravensbergen, J.; Antoniuk-Pablant, A.; Sherman, B. D.; van Grondelle, R.; Frese, R. N.; Moore, T. A.; Gust, D.; Moore, A. L.; Kennis, J. T. M. Carotenoids as Electron or Excited-State Energy Donors in Artificial Photosynthesis: An Ultrafast Investigation of a Carotenoporphyrin and a Carotenofullerene Dyad. *Phys. Chem. Chem. Phys.* **2013**, *15*, 4775−4784.
(18) Jordens, S.; De Belder, G.; Lor, M.; Schweitzer, G.; Van der Auweraer, M.; Weil, T.; Reuther, E.; Mullen, L.; De Schryver, F. C. Energy Transfer within Perylene-Terrylene Dendrimers Evidenced by Polychromatic Transient Absorption Measurements. *Photochem. Photobiol. Sci.* **2003**, *2*, 177−186.
(19) Bautista, J. A.; Hiller, R. G.; Sharples, F. P.; Gosztola, D.; Wasielewski, M.; Frank, H. A. Singlet and Triplet Energy Transfer in the Peridinin- Chlorophyll a Protein from Amphidinium Carterae. *J. Phys. Chem. A* **1999**, *103*, 2267−2273.
(20) van Stokkum, I. H. M.; Papagiannakis, E.; Vengris, M.; Salverda, J. M.; Polivka, T.; Zigmantas, D.; Larsen, D. S.; Lampoura, S. S.; Hiller, R. G.; van Grondelle, R. Inter-Pigment Interactions in the Peridinin Chlorophyll Protein Studied by Global and Target Analysis of Time Resolved Absorption Spectra. *Chem. Phys.* **2009**, *357*, 70−78.
(21) Berera, R.; Herrero, C.; van Stokkum, L. H. M.; Vengris, M.; Kodis, G.; Palacios, R. E.; van Amerongen, H.; van Grondelle, R.; Gust, D.; Moore, T. A.; et al. A Simple Artificial Light-Harvesting Dyad as a Model for Excess Energy Dissipation in Oxygenic Photosynthesis. *Proc. Natl. Acad. Sci. U.S.A.* **2006**, *103*, 5343−5348.
(22) Papagiannakis, E.; Vengris, M.; Valkunas, L.; Cogdell, R. J.; van Grondelle, R.; Larsen, D. S. Excited-State Dynamics of Carotenoids in Light-Harvesting Complexes. 2. Dissecting Pulse Structures from Optimal Control Experiments. *J. Phys. Chem. B* **2006**, *110*, 5737−5746.
(23) Nakamura, R.; Nakagawa, K.; Nango, M.; Hashimoto, H.; Yoshizawa, M. Dark Excited States of Carotenoid Regulated by Bacteriochlorophyll in Photosynthetic Light Harvesting. *J. Phys. Chem. B* **2011**, *115*, 3233−3239.
(24) Kennis, J. T. M.; Larsen, D. S.; van Stokkum, N. H. M.; Vengris, M.; van Thor, J. J.; van Grondelle, R. Uncovering the Hidden Ground State of Green Fluorescent Protein. *Proc. Natl. Acad. Sci. U.S.A.* **2004**, *101*, 17988−17993.
(25) Larsen, D. S.; van Stokkum, I. H. M.; Vengris, M.; van der Horst, M. A.; de Weerd, F. L.; Hellingwerf, K. J.; van Grondelle, R. Incoherent Manipulation of the Photoactive Yellow Protein Photocycle with Dispersed Pump-Dump-Probe Spectroscopy. *Biophys. J.* **2004**, *87*, 1858−1872.
(26) Larsen, D. S.; Vengris, M.; van Stokkum, I. H. M.; van der Horst, M. A.; de Weerd, F. L.; Hellingwerf, K. J.; van Grondelle, R. Photoisomerization and Photoionization of the Photoactive Yellow Protein Chromophore in Solution. *Biophys. J.* **2004**, *86*, 2538−2550.
(27) Hofmann, E.; Wrench, P. M.; Sharples, F. P.; Hiller, R. G.; Welte, W.; Diederichs, K. Structural Basis of Light Harvesting by Carotenoids: Peridinin- Chlorophyll-Protein from Amphidinium Carterae. *Science* **1996**, *272*, 1788−1791.
(28) Koradi, R.; Billeter, M.; Wuthrich, K. Molmol: A Program for Display and Analysis of Macromolecular Structures. *J. Mol. Graphics* **1996**, *14*, 51−&.
(29) Gradinaru, C. C.; van Stokkum, I. H. M.; Pascal, A. A.; van Grondelle, R.; van Amerongen, H. Identifying the Pathways of Energy Transfer between Carotenoids and Chlorophylls in Lhcii and Cp29. A Multicolor Pump-Probe Study. *J. Phys. Chem. B* **2000**, *104*, 9330−9342.
(30) Larsen, D. S.; Vengris, M.; van Stokkum, I. H. M.; van der Horst, M.; de Weerd, F. L.; Hellingwerf, K. J.; van Grondelle, R. Photoisomerization and Photoionization of the Photoactive Yellow Protein Chromophore in Solution. *Biophys. J.* **2004**, *86*, 2538−2550.
(31) Marino-Ochoa, E.; Palacios, R.; Kodis, G.; Macpherson, A. N.; Gillbro, T.; Gust, D.; Moore, T. A.; Moore, A. L. High-Efficiency Energy Transfer from Carotenoids to a Phthalocyanine in an Artificial Photosynthetic Antenna. *Photochem. Photobiol.* **2002**, *76*, 116−121.
(32) Krueger, B. P.; Lampoura, S. S.; van Stokkum, I. H. M.; Papagiannakis, E.; Salverda, J. M.; Gradinaru, C. C.; Rutkauskas, D.; Hiller, R. G.; van Grondelle, R. Energy Transfer in the Peridinin Chlorophyll-a Protein of Amphidinium Carterae Studied by Polarized Transient Absorption and Target Analysis. *Biophys. J.* **2001**, *80*, 2843−2855.
(33) Zigmantas, D.; Hiller, R. G.; Sundstrom, V.; Polivka, T. Carotenoid to Chlorophyll Energy Transfer in the Peridinin-Chlorophyll-a-Protein Complex Involves an Intramolecular Charge Transfer State. *Proc. Natl. Acad. Sci. U.S.A.* **2002**, *99*, 16760−16765.
(34) Zigmantas, D.; Hiller, R. G.; Yartsev, A.; Sundström, V.; Polívka, T. Dynamics of Excited States of the Carotenoid Peridinin in Polar Solvents: Dependence on Excitation Wavelength, Viscosity, and Temperature. *J. Phys. Chem. B* **2003**, *107*, 5339.
(35) Demidov, A. A. Use of a Monte Carlo Method in the Problem of Energy Migration in Molecular Complexes. In *Resonance Energy Transfer*; Andrews, D. L., Demidov, A. A., Eds.; J. Wiley and Sons: Chichester, U.K., 1999; pp 437−465.
(36) Zigmantas, D.; Polivka, T.; Hiller, R. G.; Yartsev, A.; Sundstrom, V. Spectroscopic and Dynamic Properties of the Peridinin Lowest Singlet Excited States. *J. Phys. Chem. A* **2001**, *105*, 10296−10306.
(37) Polivka, T.; Sundstrom, V. Ultrafast Dynamics of Carotenoid Excited States - from Solution to Natural and Artificial Systems. *Chem. Rev.* **2004**, *104*, 2021.

(38) Press, W. H.; Flannery, B. P.; Teukolsky, S. A.; Vetterling, W. T. *Numerical Recipes in C*, 2nd ed.; Cambridge University Press: Cambridge, U.K., 1993.
(39) Holzwarth, A. R. Data Analysis in Time-Resolved Measurements. In *Biophysical Techniques in Photosynthesis*; Amesz, J., Hoff, A. J., Eds.; Kluwer: Dordrecht, The Netherlands, 1996.
(40) van Stokkum, I. H. M.; Larsen, D. S.; van Grondelle, R. Global and Target Analysis of Time-Resolved Spectra. *Biochim. Biophys. Acta, Bioenerg.* **2004**, *1657*, 82−104.
(41) Berera, R.; van Stokkum, I. H. M.; Kodis, G.; Keirstead, A. E.; Pillai, S.; Herrero, C.; Palacios, R. E.; Vengris, M.; van Grondelle, R.; Gust, D.; et al. Energy Transfer, Excited-State Deactivation, and Exciplex Formation in Artificial Caroteno-Phthalocyanine Light-Harvesting Antennas. *J. Phys. Chem. B* **2007**, *111*, 6868−6877.
(42) Polivka, T.; Sundstrom, V. Ultrafast Dynamics of Carotenoid Excited States - from Solution to Natural and Artificial Systems. *Chem. Rev.* **2004**, *104*, 2021−2071.
(43) Polivka, T.; van Stokkum, I. H. M.; Zigmantas, D.; van Grondelle, R.; Sundstrom, V.; Hiller, R. G. Energy Transfer in the Major Intrinsic Light-Harvesting Complex from Amphidinium Carterae. *Biochemistry* **2006**, *45*, 8516−8526.
(44) Zigmantas, D.; Hiller, R. G.; Sundstrom, V.; Polivka, T. Carotenoid to Chlorophyll Energy Transfer in the Peridinin-Chlorophyll-a-Protein Complex Involves an Intramolecular Charge Transfer State. *Proc. Natl. Acad. Sci. U.S.A.* **2002**, *99*, 16760−16765.
(45) Polivka, T.; Hiller, R. G.; Frank, H. A. Spectroscopy of the Peridinin-Chlorophyll-a Protein: Insight into Light-Harvesting Strategy of Marine Algae. *Arch. Biochem. Biophys.* **2007**, *458*, 111−120.
(46) Gradinaru, C. C.; Kennis, J. T. M.; Papagiannakis, E.; van Stokkum, I. H. M.; Cogdell, R. J.; Fleming, G. R.; Niederman, R. A.; van Grondelle, R. An Unusual Pathway of Excitation Energy Deactivation in Carotenoids: Singlet-to-Triplet Conversion on an Ultrafast Timescale in a Photosynthetic Antenna. *Proc. Natl. Acad. Sci. U.S.A.* **2001**, *98*, 2364−2369.
(47) Shiu, Y. J.; Shi, Y.; Hayashi, M.; Su, C.; Han, K. L.; Lin, S. H. Femtosecond Spectroscopy Study of Electronically Excited States of Chlorophyll a Molecules in Ethanol. *Chem. Phys. Lett.* **2003**, *378*, 202−210.
(48) Ilagan, R. P.; Shima, S.; Melkozernov, A.; Lin, S.; Blankenship, R. E.; Sharples, F. P.; Hiller, R. G.; Birge, R. R.; Frank, H. A. Spectroscopic Properties of the Main-Form and High-Salt Peridinin-Chlorophyll a Proteins from Amphidinium Carterae. *Biochemistry* **2004**, *43*, 1478−1487.
(49) Jimenez, R.; Fleming, G. R.; Kumar, P. V.; Maroncelli, M. Femtosecond Solvation Dynamics of Water. *Nature* **1994**, *369*, 471−473.
(50) Kovalenko, S. A.; Ernsting, N. P.; Ruthmann, J. Femtosecond Stokes Shift in Styryl Dyes: Solvation or Intramolecular Relaxation? *J. Chem. Phys.* **1997**, *106*, 3504−3511.
(51) Kovalenko, S. A.; Schanz, R.; Hennig, H.; Ernsting, N. P. Cooling Dynamics of an Optically Excited Molecular Probe in Solution from Femtosecond Broadband Transient Absorption Spectroscopy. *J. Chem. Phys.* **2001**, *115*, 3256−3273.
(52) Jordanides, X. J.; Lang, M. J.; Song, X. Y.; Fleming, G. R. Solvation Dynamics in Protein Environments Studied by Photon Echo Spectroscopy. *J. Phys. Chem. B* **1999**, *103*, 7995−8005.
(53) Castner, E. W., Jr.; Maroncelli, M. Solvent Dynamics Derived from Optical Kerr Effect, Dielectric Dispersion, and Time-Resolved Stokes Shift Measurements: A Empirical Comparison. *J. Mol. Liq.* **1998**, *77*, 1−36.
(54) Papagiannakis, E.; Kennis, J. T. M.; van Stokkum, I. H. M.; Cogdell, R. J.; van Grondelle, R. An Alternative Carotenoid-to-Bacteriochlorophyll Energy Transfer Pathway in Photosynthetic Light Harvesting. *Proc. Natl. Acad. Sci. U.S.A.* **2002**, *99*, 6017−6022.
(55) Shepanski, J. F.; Anderson, R. W. Chlorophyll-a Excited Singlet-State Absorption Measured in the Picosecond Time Regime. *Chem. Phys. Lett.* **1981**, *78*, 165−173.